Cell Metabolism
Short Article

Reduced Apoptosis and Plaque Necrosis in Advanced Atherosclerotic Lesions of *Apoe*−/− and *Ldlr*−/− Mice Lacking CHOP

Edward Thorp,[1,5] Gang Li,[1,5] Tracie A. Seimon,[1] George Kuriakose,[1] David Ron,[4] and Ira Tabas[1,2,3,*]
[1]Department of Medicine
[2]Department of Pathology and Cell Biology
[3]Department of Physiology and Cellular Biophysics
Columbia University, New York, NY 10032, USA
[4]Skirball Institute, New York University Medical Center, 540 First Avenue, New York, NY 10016, USA
[5]These authors contributed equally to this work
*Correspondence: iat1@columbia.edu
DOI 10.1016/j.cmet.2009.03.003

SUMMARY

Endoplasmic reticulum (ER) stress is a hallmark of advanced atherosclerosis, but its causative role in plaque progression is unknown. In vitro studies have implicated the ER stress effector CHOP in macrophage apoptosis, a process involved in plaque necrosis in advanced atheromata. To test the effect of CHOP deficiency in vivo, aortic root lesions of fat-fed *Chop*+/+;*Apoe*−/− and *Chop*−/−;*Apoe*−/− mice were analyzed for size and morphology. Despite similar plasma lipoproteins, lesion area was 35% smaller in *Chop*−/−;*Apoe*−/− mice. Most importantly, plaque necrosis was reduced by ~50% and lesional apoptosis by 35% in the CHOP-deficient mice. Similar results were found in fat-fed *Chop*−/−;*Ldlr*−/− versus *Chop*+/+;*Ldlr*−/− mice. Thus, CHOP promotes plaque growth, apoptosis, and plaque necrosis in fat-fed *Apoe*−/− and *Ldlr*−/− mice. These data provide direct evidence for a causal link between the ER stress effector CHOP and plaque necrosis and suggest that interventions weakening this arm of the UPR may lessen plaque progression.

INTRODUCTION

Understanding how asymptomatic atherosclerotic lesions are converted into plaques that are at high risk to trigger acute lumenal thrombosis is a major goal of molecular cardiology. These so-called "vulnerable" plaques are characterized by large necrotic cores, focal thinning of the fibrous cap, a high level of inflammatory cytokines and matrix proteases, and apoptosis of intimal cells (Libby et al., 1996; Kolodgie et al., 2004; Clarke and Bennett, 2006). This latter process is critical, because advanced lesional macrophage apoptosis, coupled with defective phagocytic clearance, results in postapoptotic necrosis (Tabas, 2005; Schrijvers et al., 2007). Likewise, smooth muscle cell apoptosis can lead to fibrous cap thinning (Clarke and Bennett, 2006), and endothelial apoptosis may promote a prothrombotic state and vascular dysfunction (Choy et al., 2001).

Recent studies in vitro have implicated a signal transduction pathway called the unfolded protein response (UPR) in the death of all three cell types. The UPR is normally a repair pathway that responds to a variety of perturbations that affect endoplasmic reticulum (ER) homeostasis (Kaufman, 2002; Ron, 2002; Ma and Hendershot, 2001). However, a particular branch of the UPR involving the transcription factor CHOP (GADD153) can trigger apoptosis in the setting of severe or prolonged ER stress (Zinszner et al., 1998; Feng et al., 2003a; Lin et al., 2007). Over the last several years, mechanistic studies with cultured cells and analyses of mRNA and protein expression in murine and human atheromata have suggested roles for the UPR in general and CHOP in particular in intimal cell apoptosis (Feng et al., 2003a, 2003b; Hossain et al., 2003; Zhou et al., 2005; Gargalovic et al., 2006; Myoishi et al., 2007; Pedruzzi et al., 2004; Sanson et al., 2009). For example, CHOP plays a role in macrophage apoptosis induced by combinations of ER stressors and pattern recognition receptor (PRR) ligand (Feng et al., 2003a; DeVries-Seimon et al., 2005). In these studies, deletion of CHOP blocked apoptosis without leading to "default" necrosis (Feng et al., 2003a). In vivo significance is suggested by studies showing elevated levels of mRNA and protein of UPR effectors, including CHOP, in advanced murine aortic root and human coronary artery plaques (Feng et al., 2003a; Zhou et al., 2005; Gargalovic et al., 2006; Myoishi et al., 2007; Sanson et al., 2009). For example, Myoishi et al. found a very strong correlation between expression of UPR markers, including CHOP, and plaque necrosis and rupture in human coronary artery lesions (Myoishi et al., 2007). In this regard, a large number of molecules or processes that are known to exist in advanced plaques are UPR inducers, including oxidized lipids, homocysteine, oxidative stress, and insulin resistance (Gargalovic et al., 2006; Hossain et al., 2003; Han et al., 2006).

Despite this large body of correlative data, there are no studies testing the causal relationship between CHOP expression and the development of atherosclerotic lesions in vivo. Here, we report that advanced aortic root lesions of both *Chop*−/−;*Apoe*−/− mice and *Chop*−/−;*Ldlr*−/− fed an atherogenic diet are smaller in total area and, most importantly, have substantially

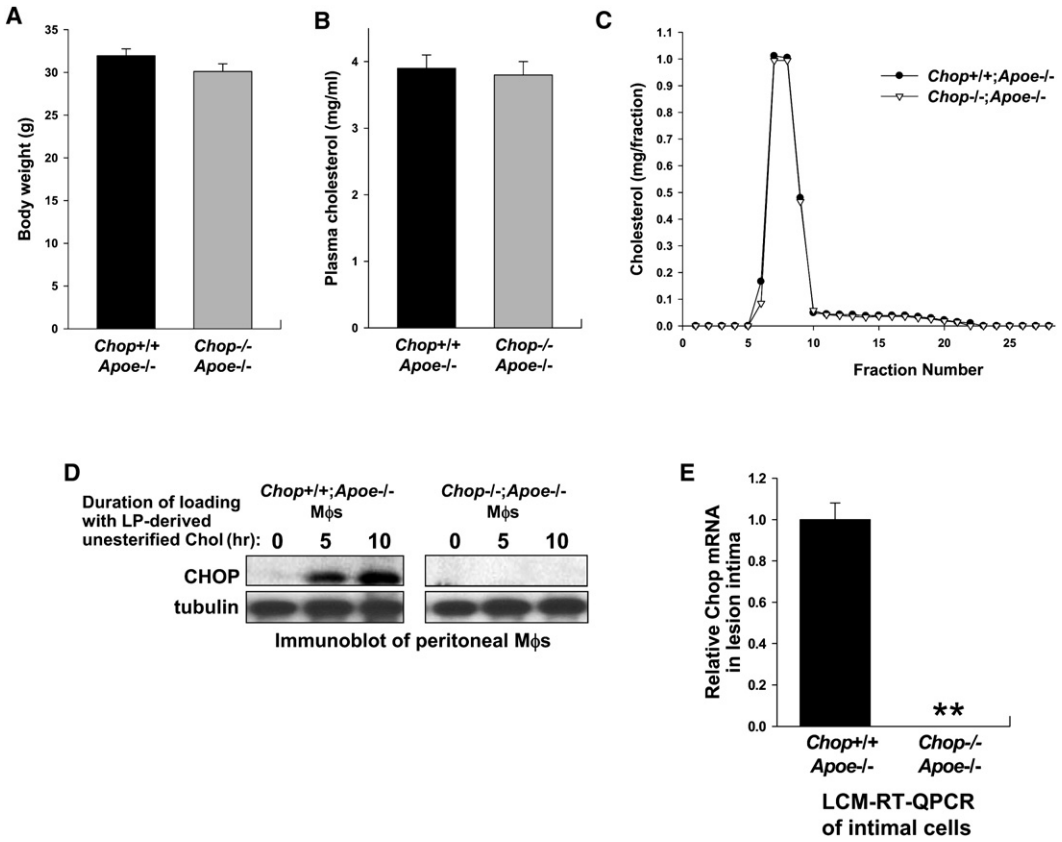

Figure 1. Total Body Weight, Plasma Lipoproteins, and CHOP Expression in *Chop*+/+;*Apoe*−/− and *Chop*−/−;*Apoe*−/− Mice

(A and B) Body weight and total plasma cholesterol of Western diet-fed male *Chop*+/+;*Apoe*−/− and *Chop*−/−;*Apoe*−/− mice (n = 20 and 21, respectively).

(C) Pooled plasma samples were subjected to fast performance liquid chromatography gel filtration, and the fractions were assayed for cholesterol concentration. None of the differences between the two groups of mice in (A)–(C) were statistically significant.

(D) Peritoneal macrophages from *Chop*+/+;*Apoe*−/− and *Chop*−/−;*Apoe*−/− mice were loaded with lipoprotein-derived unesterified cholesterol for the indicated times, and then whole-cell lysates were subjected to immunoblot analysis for CHOP and, as a loading control, tubulin.

(E) RNA from the intima of aortic root lesions of *Chop*+/+;*Apoe*−/− and *Chop*−/−;*Apoe*−/− mice (Figure 2) was captured by LCM, and *Chop* and *Cypa* mRNA were quantified by RT-QPCR. Relative expression was normalized to *Cypa*. Results are displayed as the mean ± SEM (n = 3 RT-PCR replicates). **, *Chop* mRNA not detected. Error bars indicate standard errors.

diminished plaque necrosis and less intimal cell apoptosis than the lesions of these mice with normal CHOP expression.

RESULTS

Chop+/+;*Apoe*−/− and *Chop*−/−;*Apoe*−/− mice on the C57BL6 background were placed on a Western-type diet at age 8 weeks and maintained on this diet for an additional 10 weeks. The mice were then sacrificed and analyzed for lipoprotein, metabolic, and plaque characteristics. As shown in Figures 1A–1C, the two groups of mice did not differ significantly in body weight, total plasma cholesterol, or fasting lipoprotein profile. Moreover, plasma triglycerides, glucose, and insulin did not differ significantly between the two groups of mice (data not shown). As expected, peritoneal macrophages from the *Chop*+/+;*Apoe*−/− mice expressed CHOP when loaded with lipoprotein-derived unesterified cholesterol (Feng et al., 2003a), while macrophages from the *Chop*−/−;*Apoe*−/− did not (Figure 1D). To determine CHOP expression in plaques, we quantified *Chop* mRNA using RT-QPCR of samples obtained by laser capture microdissection (LCM) of nonendothelial intimal cells. On average, greater than 70% of the intimal cells were F4/80-positive macrophages. This technique was used because CHOP immunohistochemistry gives nonspecific staining in atheromata (I.T. and C. Devlin, unpublished data). As shown in Figure 1E, *Chop* mRNA was readily detected in the lesions of *Chop*+/+;*Apoe*−/− mice but not in the lesions of *Chop*−/−;*Apoe*−/− mice.

Atherosclerotic lesions were analyzed at the aortic root. As shown in the representative images and quantitative data in Figure 2A, lesion area was 35% less in *Chop*−/−;*Apoe*−/− mice compared with *Chop*+/+;*Apoe*−/− mice ($p < 0.05$). In vitro, macrophages from *Chop*+/− mice were equally susceptible to FC-induced apoptosis as those from *Chop*+/+ mice (I.T. and B. Feng, unpublished data). Consistent with these findings, aortic root lesion area of *Apoe*−/−;*Chop*+/+ and *Apoe*−/−;*Chop*+/− mice were statistically indistinguishable (data not shown).

In human atherosclerotic cardiovascular disease, plaque morphology is a more important predictor of plaque disruption and acute clinical events than plaque size (Brown et al., 1993). In particular, the size of the necrotic core of advanced plaques

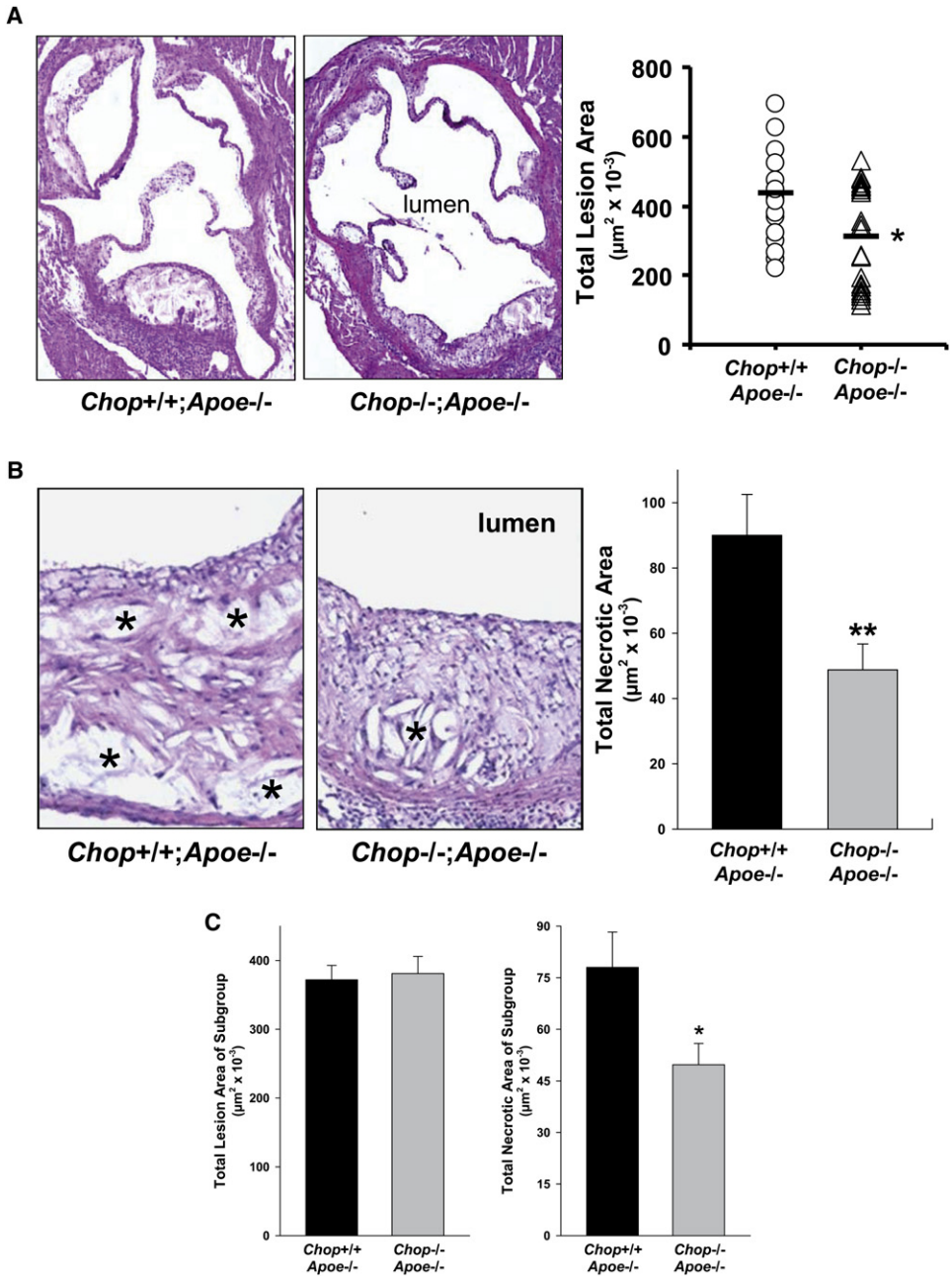

Figure 2. Reduction in Aortic Root Lesion Area and Necrotic Area in *Chop*−/−;*Apoe*−/− Mice

(A) The images show representative sections of aortic roots from each group of mice stained with hematoxylin and eosin. Quantification was conducted on lesions from 20 *Chop*+/+;*Apoe*−/− mice and 21 *Chop*−/−;*Apoe*−/− mice. *, p = 0.03.

(B) Representative sections of hematoxylin and eosin-stained aortic root sections from *Chop*+/+;*Apoe*−/− and *Chop*−/−;*Apoe*−/− mice (* = necrotic areas). The bar graph shows quantification of anuclear, afibrotic, and eosin-negative necrotic areas (n = 20 for both groups of mice). **, p < 0.01.

(C) Quantification of necrotic area in a subgroup of 12 *Chop*+/+;*Apoe*−/− lesions and 10 *Chop*−/−;*Apoe*−/− lesions with statistically identical lesion area. *, p = 0.039. Error bars indicate standard errors.

is a key determinant of plaque vulnerability (Brown et al., 1993; Kolodgie et al., 2004). Analysis of lesions for acellular nonfibrotic areas revealed a clear decrease in plaque necrosis in the *Chop*−/− lesions, and quantification of this parameter for the entire cohort of mice indicated a 46% decrease in total necrotic area in the lesions of *Chop*−/−;*Apoe*−/− mice (p < 0.01) (Figure 2B). To control for the potentially confounding influence of the decrease in lesion area, we carried out a subgroup analysis of 12 *Chop*+/+;*Apoe*−/− lesions and 10 *Chop*−/−;*Apoe*−/− lesions with statistically identical lesion area. In this subgroup, the *Chop*−/−;*Apoe*−/− lesions had a 36% decrease in necrosis (p = 0.039) (Figure 2C).

The decreased plaque necrosis in *Chop*−/−;*Apoe*−/− atheromata could reflect a primary decrease in macrophage apoptosis and/or increased efficiency of phagocytic clearance of the apoptotic cells (efferocytosis) in *Chop*−/−;*Apoe*−/− lesions (Tabas, 2005; Schrijvers et al., 2007). Consistent with our previous study (Feng et al., 2003a), macrophages from *Chop*−/−;*Apoe*−/− mice showed a 71% protection from apoptosis induced by loading the macrophages with lipoprotein-derived unesterified cholesterol ($p < 0.01$) (Figure 3A, left graph). Similar results were found with 7-ketocholesterol (Figure 3A, middle graph), an oxysterol and ER stressor present in advanced atheromata (Myoishi et al., 2007; Sanson et al., 2009). To test an ER stress-PRR combination known to be present in atheromata, we incubated macrophages with SIN-1, which generates peroxynitrite and induces ER stress in cells (Kawahara et al., 2001; Dickhout et al., 2005), and low-dose oxidized LDL, which is a PRR ligand (Miller et al., 2003). At the doses used, neither SIN-1 nor oxidized LDL alone triggered apoptosis in macrophages (Figure 3A, right graph). However, the combination was a potent inducer of apoptosis, and apoptosis was markedly reduced in macrophages from CHOP-deficient mice. Regarding efferocytosis, there was no statistically significant difference in the ability of *Chop*+/+;*Apoe*−/− versus *Chop*−/−;*Apoe*−/− macrophages to engulf apoptotic macrophages, regardless of whether the apoptotic cells were from either type of mouse (Figure 3B). Pending assessment of efferocytosis in vivo, these combined data are consistent with the interpretation that decreased susceptibility to apoptosis is a cause of decreased plaque necrosis in *Chop*−/−;*Apoe*−/− lesions.

To directly assess apoptosis in situ, lesions from the two groups of mice were stained by the TUNEL method to detect apoptotic cells (Kockx, 1998). The representative images in Figure 3C show occasional TUNEL-positive nuclei, at the expected low frequency, in *Chop*+/+;*Apoe*−/− lesions (Kockx, 1998; Feng et al., 2003b). Most importantly, lesions from *Chop*−/−;*Apoe*−/− mice had 35% less TUNEL-positive nuclei than lesions from *Chop*+/+;*Apoe*−/− mice ($p < 0.01$) (graph in Figure 3C). Similar data were obtained using activated caspase-3 as an assay for lesional apoptosis (Figure 3D). The less robust effect of CHOP deficiency shown here compared with the cell culture studies above likely reflects the difficultly of assessing cumulative apoptotic events in vivo (see Discussion). Cellular immunostaining showed that many of the TUNEL-positive nuclei were in macrophage-rich regions (Figure 3E), and quantification revealed that 78% of these apoptotic cells colocalized with macrophages in *Chop*+/+;*Apoe*−/− lesions and 72% in *Chop*−/−;*Apoe*−/− lesions ($p > 0.05$) . These combined mechanistic and lesional data are consistent with the hypothesis that decreased macrophage apoptosis conferred by CHOP deficiency contributes, at least in part, to a reduction in advanced lesional plaque necrosis.

To test the effect of CHOP deficiency in a different model of advanced atherosclerosis, *Chop*+/+;*Ldlr*−/− and *Chop*−/−;*Ldlr*−/− mice were fed the Western diet for 12 weeks, and the aortic root was analyzed for overall lesion size, plaque necrosis, and TUNEL-positive cells. Fortunately, body weight, lipoprotein levels, and lipoprotein distribution did not differ between the *Chop*+/+ and *Chop*−/− *Ldlr*−/− mice (Figure 4A). Overall lesion area was modestly lower in the CHOP-deficient mice, but necrotic area was decreased more substantially (Figure 4B). TUNEL-positive nuclei and activated caspase-3-positive cells were significantly less abundant in the macrophage-rich intimal of the lesions of the CHOP-deficient mice (Figures 4C and 4D). Thus, CHOP deficiency in the two most widely studied models of murine atherosclerosis show strikingly similar effects: modest reduction in lesion area with more substantial reduction in both plaque necrosis and intimal apoptosis.

DISCUSSION

In humans, advanced necrotic atheromata are responsible for acute atherothrombotic clinical events. While the mouse is not a good model for plaque disruption and acute atherothrombosis (Rosenfeld et al., 2002), it is a reasonable model for plaque necrosis (Tabas, 2008). Therefore, understanding processes that promote plaque necrosis in mice may give insight into plaque disruption and atherothrombosis in humans. The data herein with two separate models of advanced murine atherosclerosis, together with correlative findings with advanced human coronary atheromata (Gargalovic et al., 2006; Myoishi et al., 2007), suggest that the CHOP branch of the UPR contributes significantly to advanced atherosclerotic plaque progression. While it is theoretically possible that CHOP affects macrophage apoptosis plus a nonapoptotic process involved in plaque necrosis per se, we hypothesize that the decrease in plaque necrosis is a direct consequence of the decrease in apoptosis in the CHOP-deficient mice. This hypothesis is based upon the concept that in advanced atheromata, where efferocytosis appears to be defective, apoptosis becomes rate-limiting for postapoptotic necrosis (Schrijvers et al., 2005, 2007; Tabas, 2005).

The concept that CHOP plays an important role in macrophage apoptosis in advanced atherosclerotic lesions is now supported by several experimental findings: (1) the role of CHOP in apoptosis of ER-stressed cultured macrophages (Feng et al., 2003a) (Figure 3A); (2) the fact that CHOP is expressed in advanced lesional macrophages (Feng et al., 2003a; Zhou et al., 2005; Myoishi et al., 2007); and most importantly, (3) our data here showing decreased apoptosis in macrophage-rich lesional regions in two models of CHOP-deficient atherosclerosis-prone mice. Although the presence of ER stress in advanced atheromata is likely the major force behind CHOP expression, it is theoretically possible that non-ER stress activators of the phospho-eIF2α-ATF4-CHOP pathway, like amino acid starvation in deep regions of the intima, may contribute as well (Bruhat et al., 1997). Furthermore, while one might expect a somewhat greater decrease in lesional apoptotic cells based on our cell culture data, in situ measurements of apoptosis reflect the net effect of apoptosis and efferocytosis or postapoptotic necrosis rather than cumulative apoptotic events over a long period of time, and so one can only obtain an estimate of trends in one direction or another from these measurements. Finally, studies to address the role of CHOP specifically in macrophages using bone marrow transplantation is not possible due to the fact that lethal irradiation fundamentally alters the relationship between CHOP and atherosclerosis (E.T., G.L., and I.T., unpublished data). Thus, creation of *Cre-Lox* models will be necessary to address this important issue.

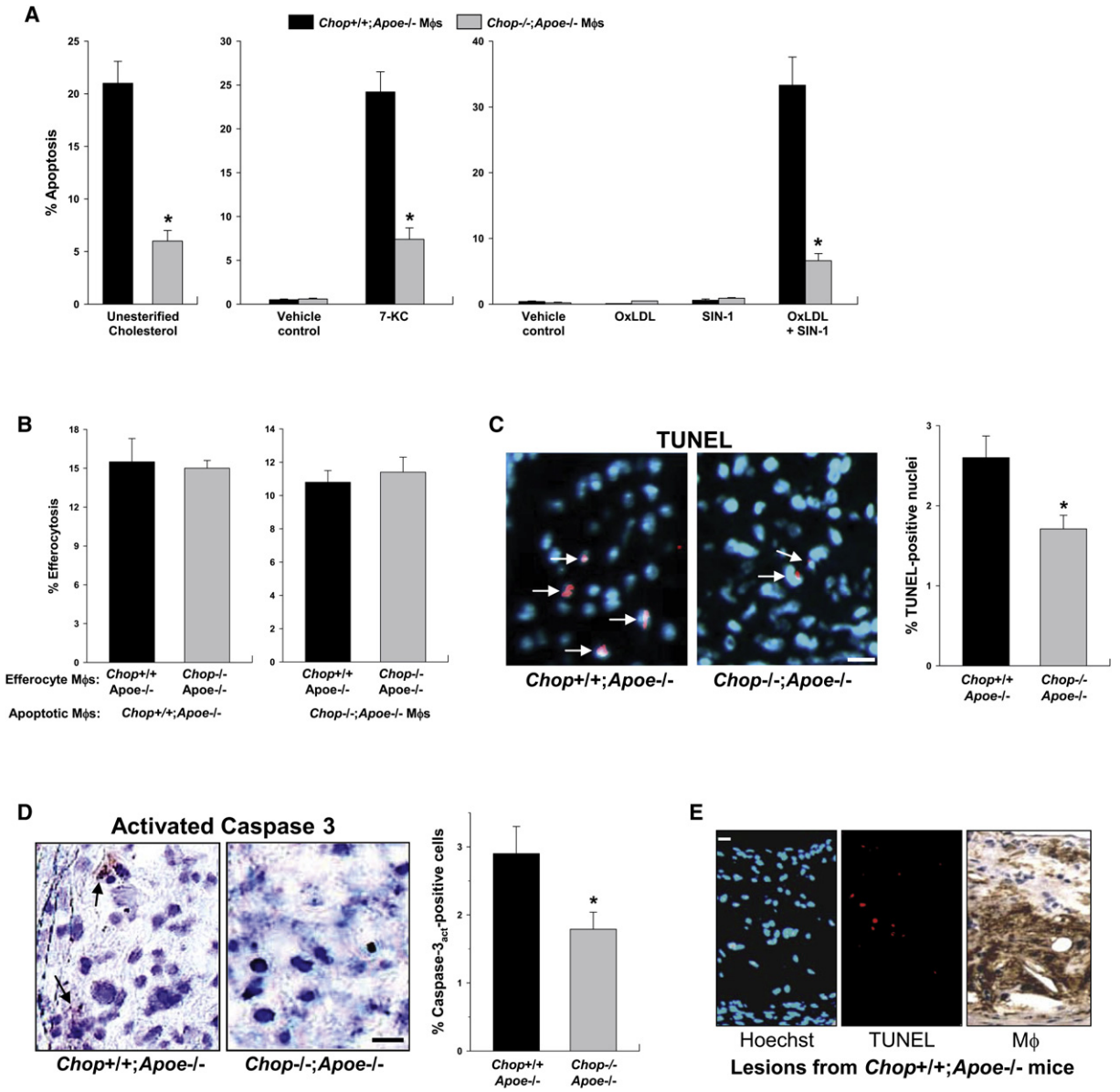

Figure 3. Reduction in Peritoneal Macrophage and Aortic Root Lesional Macrophage Apoptosis in *Apoe*−/−;*Chop*−/− Mice

(A) Left graph: macrophages from *Chop*+/+;*Apoe*−/− or *Chop*−/−;*Apoe*−/− mice were loaded with lipoprotein-derived unesterified cholesterol and then assayed for apoptosis (*, $p < 0.01$). Middle graph represents macrophages incubated for 18 hr with vehicle control (0.2% ethanol) or 50 μM 7-ketocholesterol and then assayed for apoptosis (*, $p < 0.01$ compared with *Chop*+/+;*Apoe*−/− macrophages). Right graph represents macrophages incubated for 15 hr with vehicle control, 50 μg/ml oxidized LDL (*OxLDL*), 1 mM SIN-1, or both compounds. The cells were then assayed for apoptosis (*, $p < 0.01$ compared with *Chop*+/+;*Apoe*−/− macrophages). In the case of cholesterol loading, ~5% of apoptotic cells were PI-positive. With 7-ketocholesterol and OxLDL + SIN-1, the percentage of PI-positive cells was > 50%, indicating advanced apoptosis, and both annexin-positive and PI-positive cells were decreased in the CHOP-deficient macrophages.

(B) Efferocytosis assays were conducted using various combinations of peritoneal macrophages from *Chop*+/+;*Apoe*−/− and *Chop*−/−;*Apoe*−/− mice, where the macrophages served as the source of either the apoptotic cells or the efferocytes. None of the differences shown are statistically significant.

(C) Representative micrographs show less TUNEL-positive signal (red; arrows) in nuclei (blue) of aortic root lesions from *Chop*−/−;*Apoe*−/− lesions. Bar, 10 μm. Quantification of TUNEL-positive nuclei was conducted on lesions from 20 *Chop*+/+;*Apoe*−/− mice and 21 *Chop*−/−;*Apoe*−/− mice. *, $p < 0.01$.

(D) Representative micrographs show less activated caspase-3 (red; arrows) in aortic root lesions from *Chop*−/−;*Apoe*−/− versus *Chop*−/−;*Apoe*−/− lesions. Bar, 10 μm. Quantification of TUNEL-positive cells was conducted on lesions from seven *Chop*+/+;*Apoe*−/− mice and seven *Chop*−/−;*Apoe*−/− mice. *, $p < 0.05$.

(E) Representative sequential sections of a *Chop*+/+;*Apoe*−/− lesion stained for nuclei (Hoechst), TUNEL, and macrophages. Bar, 10 μm. Error bars indicate standard errors.

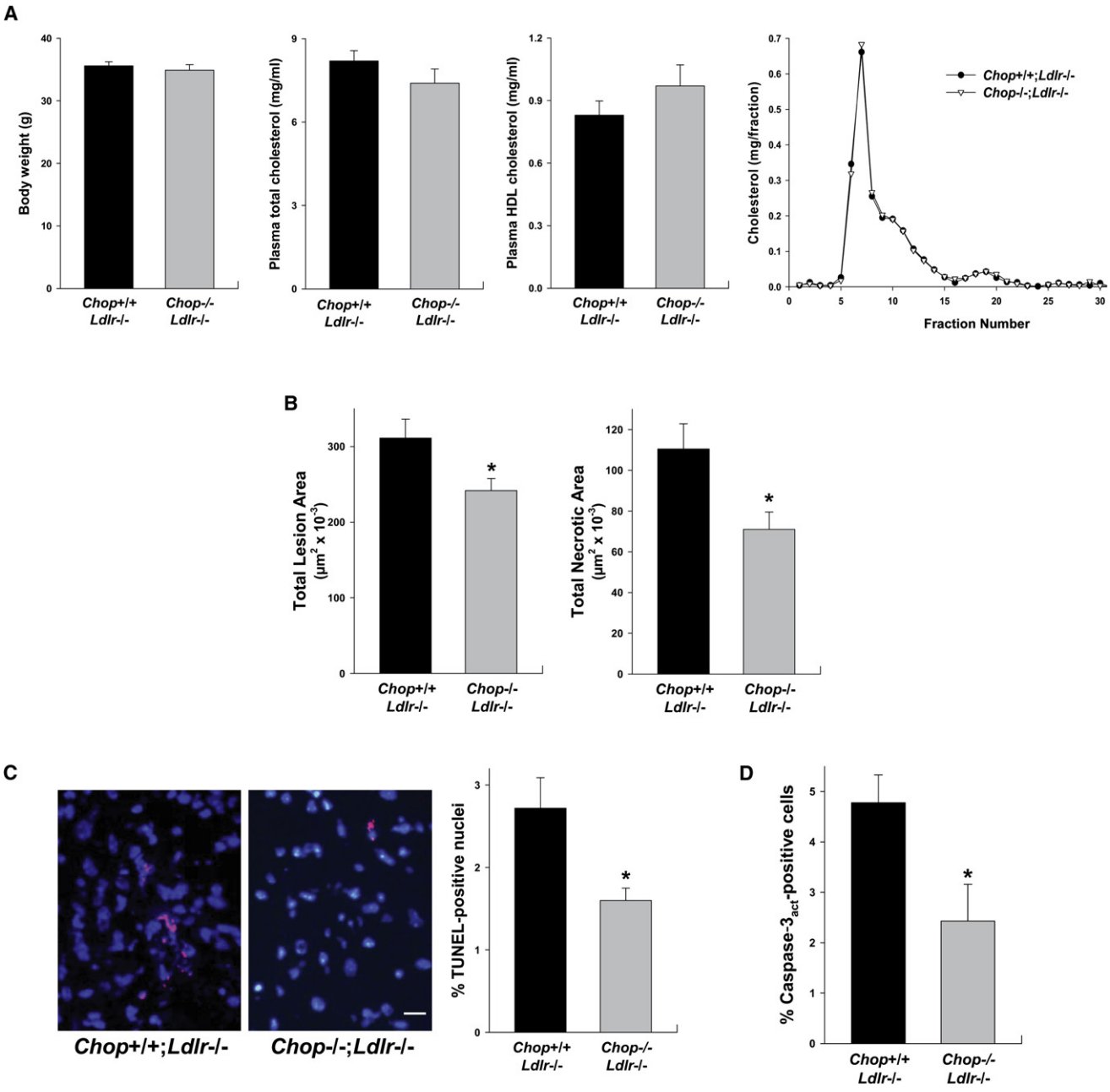

Figure 4. Reduction in Aortic Root Lesion Area, Necrotic Area, and Apoptosis in *Ldlr*−/−;*Chop*−/− Mice

(A) Body weight, plasma total cholesterol, plasma HDL cholesterol, and fast-protein liquid chromatogrpahy plasma cholesterol profile of 12 week Western diet-fed male *Chop*+/+;*Ldlr*−/− and *Chop*−/−;*Ldlr*−/− mice (n = 12 and 17, respectively). None of the differences between the two groups of mice in these parameters were statistically significant.

(B) Quantification of total aortic root lesion area and necrotic area of the mice described in (A). *, $p < 0.05$.

(C) Representative micrographs and quantification of TUNEL-positive signal (red) in nuclei (blue) of aortic root lesions from *Chop*−/−;*Ldlr*−/− lesions. Bar, 10 μm. *, $p < 0.05$.

(D) Quantification of activated caspase-3 in aortic root lesions from *Chop*+/+;*Ldlr*−/− and *Chop*−/−;*Ldlr*−/− lesions. *, $p < 0.05$. Error bars indicate standard errors.

While CHOP expression is pronounced in advanced atherosclerotic lesions, it is also expressed in early lesions, albeit in lesser amounts (Zhou et al., 2005; Myoishi et al., 2007). Using LCM-RT-QPCR, we found that *Chop* mRNA was 2.9-fold less in lesions from *Apoe*−/− mice fed the Western diet for 4 weeks versus 10 weeks (n = 3; $p < 0.05$). In the 4 week diet study, the *Chop*+/+;*Apoe*−/− and *Chop*−/−;*Apoe*−/− lesion areas were 162,961 ± 34,288 and 159,841 ± 11,861 μm^2, respectively (n = 6 per group; $p > 0.05$). These early lesions had only very small pockets of plaque necrosis, and the areas were not

statistically different between the two groups (data not shown). Thus, CHOP does not appear to play a significant role in early atherogenesis. However, the finding that CHOP deficiency did have a modest effect on lesion area in the 10 week diet lesions (Figures 2A and 4B) raises the possibility that CHOP plays a role in one or more processes that promote the expansion of lesions after they have reached the relatively early foam cell stage.

The results of this study, together with recent findings showing expression of CHOP in advanced human atherosclerotic plaques (Gargalovic et al., 2006; Myoishi et al., 2007), suggest that the CHOP pathway may be a potential therapeutic target related to the formation of dangerous atheromata. In particular, it will be interesting to determine whether so-called chemical chaperones, which have been successfully used in other animal models of UPR-associated diseases (Ozcan et al., 2006), have a beneficial effect on advanced atherosclerotic lesion progression.

EXPERIMENTAL PROCEDURES

Materials and additional methods are available in Supplemental Experimental Procedures.

Mice and Diets

Chop−/− mice (Zinszner et al., 1998) on the C57BL6/J were bred onto the *Apoe*−/− and *Ldlr*−/− C57BL6/J backgrounds to generate *Chop*+/−;*Apoe*−/− and *Chop*+/−;*Ldlr*−/− breeding pairs. According to genotyping with a fixed whole-genome panel of 768 murine single-nucleotide polymorphisms, *Chop*−/−;*Apoe*−/− mice were 97.3% C57BL6/J and *Chop*−/−;*Ldlr*−/− mice 99.1% C57BL6/J. Starting at 8 weeks of age, male progeny from these breeding pairs were fed a high-fat (21.2%), high-cholesterol (0.2%) Western-type diet (catalog #TD88137) from Harlan Teklad (Madison, WI) for 10 weeks (*Apoe*−/− study) or 12 weeks (*Ldlr*−/− study).

Macrophage Apoptosis and Efferocytosis Assays

Macrophage apoptosis was induced by one of three methods: (1) loading with lipoprotein-derived unesterified cholesterol by incubation with 100 μg/ml of acetyl-LDL plus 10 μg/ml of the ACAT inhibitor 58-035 (Yao and Tabas, 2000; Feng et al., 2003a); (2) incubation with 50 μM 7-ketocholesterol; or (3) incubation with the combination of 50 μg/ml oxidized LDL and 1 mM SIN-1. Apoptosis was measured by annexin V and propidium iodide staining as previously described (Yao and Tabas, 2000; Feng et al., 2003a). Efferocytosis was assessed as previously described (Li et al., 2006; Thorp et al., 2008). Briefly, macrophages were labeled for 1 hr with the fluorescent green vital stain calcein AM and then rendered apoptotic by loading with lipoprotein-derived unesterified cholesterol (above). Based upon quantification of annexin V-positivity in parallel plates, the apoptotic macrophages were added to monolayers of unloaded macrophages ("efferocytes") at a ratio of 1:1. After 45 min of coculture, the noningested apoptotic cells were removed and the ingested apoptotic cells quantified as described (Li et al., 2006).

Atherosclerotic Lesion Analysis

Mouse hearts were perfused in situ with saline and removed. Aortic roots were fixed in 10% formalin, placed in biopsy cassettes, and processed in a Leica tissue-processing machine followed by embedment in paraffin blocks. Paraffin-embedded sections were cut serially at 6 μm intervals from the aortic sinus and mounted on slides. Prior to section staining, sections were deparaffinized in xylene and rehydrated in graded series of ethanol. For area measurements and morphometric analysis, the sections were stained with Harris hematoxylin and eosin. Total intimal lesional area was quantified by averaging six sections that were spaced 30 μm apart, starting from the base of the aortic root. Images were viewed and captured with a Nikon Labophot 2 Microscope and analyzed using Image-Pro Plus software. Apoptotic cells in lesions were detected by TUNEL after proteinase K treatment, using the In Situ Cell Death Detection Kit, TMR red (Roche). Nuclei were counterstained with Hoechst for 5 min, and the slides were viewed and imaged by fluorescent microscopy. Apoptotic cells in lesions were also detected by immunostaining for activated caspase-3 using rabbit anti-cleaved caspase-3 antibody #9661 from Cell Signaling Technology. The sections were then incubated for 30 min with horseradish peroxidase-avidin conjugate using ABC Kit (Vector Laboratories), developed with substrate diaminobenzidine, and then counterstained with hematoxylin. Plaque necrosis was quantified by measuring the area of hematoxylin and eosin-negative acellular areas in the intima, as described previously (Feng et al., 2003b). For macrophage staining, the sections were heated in an EDTA solution, and then endogenous peroxidase was blocked using hydrogen peroxide and methanol. Antigen blocking was performed using immunoglobulin from the species of the secondary antibody. The sections were then incubated with rabbit anti-macrophage antibody (AIA31240) from Accurate Chemical and Scientific Corporation (Westbury, NY), followed by incubation with biotinylated secondary antibody, streptavidin-horseradish peroxidase, and diaminobenzidine. Images were viewed and captured using a Nikon Labophot 2 Microscope equipped with a Sony CCD-Iris/RGB color video camera attached to a computerized imaging system with Image-Pro Plus 3.0 software.

SUPPLEMENTAL DATA

Supplemental Data include Supplemental Experimental Procedures and Supplemental References and can be found online at http://www.cell.com/cellmetabolism/supplemental/S1550-4131(09)00063-1.

ACKNOWLEDGMENTS

This work was supported by NIH grants HL75662 and HL57560 to I.T.; DK47119 and ES08681 to D.R.; and an American Heart Association, Heritage Affiliate, postdoctoral fellowship grant to E.T.

Received: January 7, 2009
Revised: February 21, 2009
Accepted: March 5, 2009
Published: May 5, 2009

REFERENCES

Brown, B.G., Zhao, X.Q., Sacco, D.E., and Albers, J.J. (1993). Atherosclerosis regression, plaque disruption, and cardiovascular events: a rationale for lipid lowering in coronary artery disease. Annu. Rev. Med. *44*, 365–376.

Bruhat, A., Jousse, C., Wang, X.Z., Ron, D., Ferrara, M., and Fafournoux, P. (1997). Amino acid limitation induces expression of CHOP, a CCAAT/enhancer binding protein-related gene, at both transcriptional and post-transcriptional levels. J. Biol. Chem. *272*, 17588–17593.

Choy, J.C., Granville, D.J., Hunt, D.W., and McManus, B.M. (2001). Endothelial cell apoptosis: biochemical characteristics and potential implications for atherosclerosis. J. Mol. Cell. Cardiol. *33*, 1673–1690.

Clarke, M., and Bennett, M. (2006). The emerging role of vascular smooth muscle cell apoptosis in atherosclerosis and plaque stability. Am. J. Nephrol. *26*, 531–535.

DeVries-Seimon, T., Li, Y., Yao, P.M., Stone, E., Wang, Y., Davis, R.J., Flavell, R., and Tabas, I. (2005). Cholesterol-induced macrophage apoptosis requires ER stress pathways and engagement of the type A scavenger receptor. J. Cell Biol. *171*, 61–73.

Dickhout, J.G., Hossain, G.S., Pozza, L.M., Zhou, J., Lhotak, S., and Austin, R.C. (2005). Peroxynitrite causes endoplasmic reticulum stress and apoptosis in human vascular endothelium: implications in atherogenesis. Arterioscler. Thromb. Vasc. Biol. *25*, 2623–2629.

Feng, B., Yao, P.M., Li, Y., Devlin, C.M., Zhang, D., Harding, H.P., Sweeney, M., Rong, J.X., Kuriakose, G., Fisher, E.A., et al. (2003a). The endoplasmic reticulum is the site of cholesterol-induced cytotoxicity in macrophages. Nat. Cell Biol. *5*, 781–792.

Feng, B., Zhang, D., Kuriakose, G., Devlin, C.M., Kockx, M., and Tabas, I. (2003b). Niemann-Pick C heterozygosity confers resistance to lesional

necrosis and macrophage apoptosis in murine atherosclerosis. Proc. Natl. Acad. Sci. USA *100*, 10423–10428.

Gargalovic, P.S., Gharavi, N.M., Clark, M.J., Pagnon, J., Yang, W.P., He, A., Truong, A., Baruch-Oren, T., Berliner, J.A., Kirchgessner, T.G., and Lusis, A.J. (2006). The unfolded protein response is an important regulator of inflammatory genes in endothelial cells. Arterioscler. Thromb. Vasc. Biol. *26*, 2490–2496.

Han, S., Liang, C.P., DeVries-Seimon, T., Ranalletta, M., Welch, C.L., Collins-Fletcher, K., Accili, D., Tabas, I., and Tall, A.R. (2006). Macrophage insulin receptor deficiency increases ER stress-induced apoptosis and necrotic core formation in advanced atherosclerotic lesions. Cell Metab. *3*, 257–266.

Hossain, G.S., van Thienen, J.V., Werstuck, G.H., Zhou, J., Sood, S.K., Dickhout, J.G., de Koning, A.B., Tang, D., Wu, D., Falk, E., et al. (2003). TDAG51 is induced by homocysteine, promotes detachment-mediated programmed cell death, and contributes to the cevelopment of atherosclerosis in hyperhomocysteinemia. J. Biol. Chem. *278*, 30317–30327.

Kaufman, R.J. (2002). Orchestrating the unfolded protein response in health and disease. J. Clin. Invest. *110*, 1389–1398.

Kawahara, K., Oyadomari, S., Gotoh, T., Kohsaka, S., Nakayama, H., and Mori, M. (2001). Induction of CHOP and apoptosis by nitric oxide in p53-deficient microglial cells. FEBS Lett. *506*, 135–139.

Kockx, M.M. (1998). Apoptosis in the atherosclerotic plaque: quantitative and qualitative aspects. Arterioscler. Thromb. Vasc. Biol. *18*, 1519–1522.

Kolodgie, F.D., Virmani, R., Burke, A.P., Farb, A., Weber, D.K., Kutys, R., Finn, A.V., and Gold, H.K. (2004). Pathologic assessment of the vulnerable human coronary plaque. Heart *90*, 1385–1391.

Li, Y., Gerbod-Giannone, M.C., Seitz, H., Cui, D., Thorp, E., Tall, A.R., Matsushima, G.K., and Tabas, I. (2006). Cholesterol-induced apoptotic macrophages elicit an inflammatory response in phagocytes, which is partially attenuated by the Mer receptor. J. Biol. Chem. *281*, 6707–6717.

Libby, P., Geng, Y.J., Aikawa, M., Schoenbeck, U., Mach, F., Clinton, S.K., Sukhova, G.K., and Lee, R.T. (1996). Macrophages and atherosclerotic plaque stability. Curr. Opin. Lipidol. *7*, 330–335.

Lin, J.H., Li, H., Yasumura, D., Cohen, H.R., Zhang, C., Panning, B., Shokat, K.M., Lavail, M.M., and Walter, P. (2007). IRE1 signaling affects cell fate during the unfolded protein response. Science *318*, 944–949.

Ma, Y., and Hendershot, L.M. (2001). The unfolding tale of the unfolded protein response. Cell *107*, 827–830.

Miller, Y.I., Viriyakosol, S., Binder, C.J., Feramisco, J.R., Kirkland, T.N., and Witztum, J.L. (2003). Minimally modified LDL binds to CD14, induces macrophage spreading via TLR4/MD-2, and inhibits phagocytosis of apoptotic cells. J. Biol. Chem. *278*, 1561–1568.

Myoishi, M., Hao, H., Minamino, T., Watanabe, K., Nishihira, K., Hatakeyama, K., Asada, Y., Okada, K., Ishibashi-Ueda, H., Gabbiani, G., et al. (2007). Increased endoplasmic reticulum stress in atherosclerotic plaques associated with acute coronary syndrome. Circulation *116*, 1226–1233.

Ozcan, U., Yilmaz, E., Ozcan, L., Furuhashi, M., Vaillancourt, E., Smith, R.O., Gorgun, C.Z., and Hotamisligil, G.S. (2006). Chemical chaperones reduce ER stress and restore glucose homeostasis in a mouse model of type 2 diabetes. Science *313*, 1137–1140.

Pedruzzi, E., Guichard, C., Ollivier, V., Driss, F., Fay, M., Prunet, C., Marie, J.C., Pouzet, C., Samadi, M., Elbim, C., et al. (2004). NAD(P)H oxidase Nox-4 mediates 7-ketocholesterol-induced endoplasmic reticulum stress and apoptosis in human aortic smooth muscle cells. Mol. Cell. Biol. *24*, 10703–10717.

Ron, D. (2002). Translational control in the endoplasmic reticulum stress response. J. Clin. Invest. *110*, 1383–1388.

Rosenfeld, M.E., Carson, K.G., Johnson, J.L., Williams, H., Jackson, C.L., and Schwartz, S.M. (2002). Animal models of spontaneous plaque rupture: the holy grail of experimental atherosclerosis research. Curr. Atheroscler. Rep. *4*, 238–242.

Sanson, M., Auge, N., Vindis, C., Muller, C., Bando, Y., Thiers, J.C., Marachet, M.A., Zarkovic, K., Sawa, Y., Salvayre, R., and Negre-Salvayre, A. (2009). Oxidized low-density lipoproteins trigger endoplasmic reticulum stress in vascular cells: prevention by oxygen-regulated protein 150 expression. Circ. Res. *104*, 328–336.

Schrijvers, D.M., De Meyer, G.R., Kockx, M.M., Herman, A.G., and Martinet, W. (2005). Phagocytosis of apoptotic cells by macrophages is impaired in atherosclerosis. Arterioscler. Thromb. Vasc. Biol. *25*, 1256–1261.

Schrijvers, D.M., De Meyer, G.R., Herman, A.G., and Martinet, W. (2007). Phagocytosis in atherosclerosis: Molecular mechanisms and implications for plaque progression and stability. Cardiovasc. Res. *73*, 470–480.

Tabas, I. (2005). Consequences and therapeutic implications of macrophage apoptosis in atherosclerosis: the importance of lesion stage and phagocytic efficiency. Arterioscler. Thromb. Vasc. Biol. *25*, 2255–2264.

Tabas, I. (2008). Mouse models of apoptosis and efferocytosis. Curr. Drug Targets *8*, 1288–1296.

Thorp, E., Cui, D., Schrijvers, D.M., Kuriakose, G., and Tabas, I. (2008). Mertk receptor mutation reduces efferocytosis efficiency and promotes apoptotic cell accumulation and plaque necrosis in atherosclerotic lesions of apoe−/− mice. Arterioscler. Thromb. Vasc. Biol. *28*, 1421–1428.

Yao, P.M., and Tabas, I. (2000). Free cholesterol loading of macrophages induces apoptosis involving the fas pathway. J. Biol. Chem. *275*, 23807–23813.

Zhou, J., Lhotak, S., Hilditch, B.A., and Austin, R.C. (2005). Activation of the unfolded protein response occurs at all stages of atherosclerotic lesion development in apolipoprotein E-deficient mice. Circulation *111*, 1814–1821.

Zinszner, H., Kuroda, M., Wang, X., Batchvarova, N., Lightfoot, R.T., Remotti, H., Stevens, J.L., and Ron, D. (1998). CHOP is implicated in programmed cell death in response to impaired function of the endoplasmic reticulum. Genes Dev. *12*, 982–995.